Next-Generation Grid Codes: Toward a New Paradigm for Dynamic Ancillary Services

Verena Haeberle[1], Kehao Zhuang[2], Xiuqiang He[3], Linbin Huang[2], Gabriela Hug[1], Florian Doerfler[1]

[1]*ETH Zurich* [2]*Zhejiang University* [3]*Tsinghua University*

Suggested Citation

V. Haeberle, K. Zhuang, X. He, L. Huang, G. Hug, and F. Doerfler, "Next-Generation Grid Codes: Toward a New Paradigm for Dynamic Ancillary Services," in *Proceedings of the PowerUp Conference*, 2026.

BibTeX Entry

```
@inproceedings{haeberle2026nextgeneration,
  author = {Haeberle, Verena and Zhuang, Kehao and He, Xiuqiang and Huang, Linbin
      and Hug, Gabriela and Doerfler, Florian},
  title = {Next-Generation Grid Codes: Toward a New Paradigm for Dynamic Ancillary
      Services},
  booktitle = {Proceedings of the PowerUp Conference},
  year = {2026},
}
```

Next-Generation Grid Codes: Toward a New Paradigm for Dynamic Ancillary Services

Verena Häberle†, Kehao Zhuang†, Xiuqiang He‡, Linbin Huang§, Gabriela Hug†, Florian Dörfler†

***Abstract*—This paper presents *preliminary results* toward a conceptual foundation for *Next-Generation Grid Codes (NGGCs)* based on decentralized stability and performance certification for dynamic ancillary services. The proposed NGGC framework targets two core outcomes: (i) guaranteed closed-loop stability and (ii) explicit performance assurances for power-system frequency and voltage dynamics. Stability is addressed using loop-shifting and passivity-based methods that yield local frequency-domain certificates for individual devices, enabling fully decentralized verification of the interconnected system. Performance is characterized by deriving quantitative bounds on key time-domain metrics (e.g., nadirs, rate-of-change-of-frequency (RoCoF), steady-state deviations, and oscillation damping) through frequency-domain constraints on local device behavior. The framework is non-parametric and model-agnostic, accommodating a broad class of device dynamics under mild assumptions, and provides an initial unified approach to stability and performance certification without explicit device-model parameterization. As such, these results offer a principled starting point for the development of future grid codes and control design methodologies in modern power systems.**

I. Introduction

Current grid codes for dynamic ancillary services provision with converter-based generation, such as fast frequency and voltage regulation, are predominantly specified through prescribed time-domain step responses and response-time limits. The European network code [1], for instance, defines frequency containment and voltage regulation via piecewise-linear active and reactive power curves. National codes in Finland [2] and Germany [3] similarly prescribe fast frequency reserves and synthetic inertia using power injection profiles or time constants. Although conceptually simple, these requirements are often implemented via open-loop commands or look-up tables, resulting in rigid and inefficient control. Moreover, existing codes focus mainly on grid-following operation, with only recent exceptions of including grid-forming requirements [3], and they offer no guarantees of closed-loop stability or system performance. As a result, systems that comply with current grid codes may still exhibit poor dynamic behavior or instability [4], [5].

Recent grid-code proposals [6] have begun to address closed-loop stability and performance guarantees using frequency-domain concepts. However, their scope remains limited to single-device-to-grid connections and qualitative disturbance rejection, without providing explicit bounds on key metrics such as frequency nadir or RoCoF. Related efforts to incorporate passivity requirements into grid-forming control design [7] face similar challenges, as power system networks are not inherently passive. These limitations motivate the formulation of a more general, quantitative, and practically implementable framework to specify dynamic ancillary services in future grid codes.

†Verena Häberle, Kehao Zhuang, Gabriela Hug and Florian Dörfler are with the Department of Electrical Engineering, ETH Zurich, Zurich, Switzerland. Email: {verenhae,kzhuang,hug,dorfler}@ethz.ch.

‡Xiuqiang He is with the Department of Automation, Tsinghua University, Beijing 100084, China. Email: hxe@tsinghua.edu.cn.

§ Linbin Huang is with the College of Electrical Engineering, Zhejiang University, Hangzhou 310027, China. Email: hlinbin@zju.edu.cn.

This work was supported by prize funds of the Hans-Eggenberger Award.

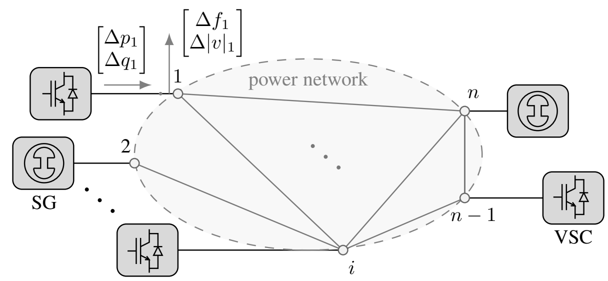

Fig. 1: Multi-device transmission system with SGs and grid-forming VSCs connected by resistive–inductive transmission lines.

This paper introduces the concept of *Next-Generation Grid Codes (NGGCs)* as a first step toward a new paradigm for dynamic ancillary services provision based on decentralized frequency-domain criteria. The NGGC framework provides two main benefits: (i) guaranteed closed-loop stability and (ii) explicit performance guarantees at the system level. For stability, we employ loop-shifting and passivity-based techniques to derive decentralized certificates that translate into local tuning rules for individual devices, ensuring modular contributions to global stability. For performance, we establish quantitative bounds on critical time-domain indicators of small-signal frequency and voltage dynamics, including frequency and voltage nadirs, RoCoF, steady-state deviations, and oscillation damping. These bounds are obtained by linking time-domain metrics to frequency-domain constraints on local device behavior and can be expressed as Nyquist-plot envelopes on device transfer functions. The framework naturally accommodates grid-forming signal causality and integrates with existing converter and synchronous-generator models.

Unlike existing decentralized stability certification methods that rely on explicit device parameterizations [4], [8], [9], the proposed approach is model-agnostic and applies to heterogeneous devices under mild behavioral assumptions. While related generic certificates based on small-gain, small-phase, or sector conditions have been reported [10], [11], the present work extends these results by simultaneously providing explicit stability and performance guarantees. To the best of our knowledge, this is the first unified framework that ensures both closed-loop stability and quantitative performance bounds for frequency and voltage dynamics under general, non-parametric device models.

II. Power System Model

Small-Signal Network Dynamics: We consider an interconnected power system composed of three-phase generation units, including grid-forming voltage-source converters (VSCs) and synchronous generators (SGs), connected through a balanced resistive–inductive transmission network. The network is represented in Kron-reduced form with n generator buses, as illustrated in Fig. 1.

The network dynamics are modeled using a quasi-stationary small-signal representation in the global per-unit system, which relates deviations in bus frequencies $\Delta f = [\Delta f_1 \dots \Delta f_n]^\top$ and voltage magnitudes $\Delta|v| = [\Delta|v|_1 \dots \Delta|v|_n]^\top$ to the corresponding active and reactive power injections $\Delta p = [\Delta p_1 \dots \Delta p_n]^\top$ and $\Delta q = [\Delta q_1 \dots \Delta q_n]^\top$. Specifically, the transmission network is described by a $2n \times 2n$ transfer matrix $N(s)$ (see [9] for a detailed derivation), such that

$$\begin{bmatrix}\Delta p(s)\\ \Delta q(s)\end{bmatrix} = \underbrace{\begin{bmatrix}N^{\mathrm{fp}}(s) & 0\\ 0 & N^{\mathrm{vq}}\end{bmatrix}}_{=:\,N(s)}\begin{bmatrix}\Delta f(s)\\ \Delta|v|(s)\end{bmatrix}, \tag{1}$$

revealing a decoupling between the active-power–frequency (pf) and reactive-power–voltage (qv) dynamics. The pf-coupling is captured by the $n \times n$ matrix $N^{\mathrm{fp}}(s)$ with entries

$$\begin{aligned} N^{\mathrm{fp}}_{ii}(s) &= \tfrac{1}{s}\tfrac{2\pi}{1+\rho^2}\textstyle\sum_{j\neq i}^{n} b_{ij}|v|_{0,i}|v|_{0,j},\\ N^{\mathrm{fp}}_{ij}(s) &= -\tfrac{1}{s}\tfrac{2\pi}{1+\rho^2} b_{ij}|v|_{0,i}|v|_{0,j}, \end{aligned} \tag{2}$$

while the qv-coupling is described by the static $n \times n$ matrix N^{vq} with elements

$$\begin{aligned} N^{\mathrm{vq}}_{ii} &= \tfrac{1}{1+\rho^2}\textstyle\sum_{j\neq i}^{n} b_{ij}\big(2|v|_{0,i} - |v|_{0,j}\big),\\ N^{\mathrm{vq}}_{ij} &= -\tfrac{1}{1+\rho^2} b_{ij}|v|_{0,i}. \end{aligned} \tag{3}$$

Here, $|v|_{0,i}$ denotes the steady-state voltage magnitude at node i, $b_{ij} = 1/l_{ij}$ is the line susceptance, and $\rho_{ij} = r_{ij}/l_{ij}$ is the resistance-to-inductance ratio of line ij. The network is assumed to be dominantly inductive, with a small and uniform $\rho_{ij} = \rho \ll 1$. If no line connects nodes i and j, we set $b_{ij} = \rho_{ij} = 0$.

Small-Signal Device Dynamics: We model generation units with grid-forming signal causality, i.e., devices that regulate frequency and voltage outputs based on measured active and reactive power deviations. The linearized dynamics of the i-th device are described by a diagonal 2×2 transfer matrix

$$-\begin{bmatrix}\Delta f_i(s)\\ \Delta|v|_i(s)\end{bmatrix} = \begin{bmatrix}D^{\mathrm{pf}}_i(s) & 0\\ 0 & D^{\mathrm{qv}}_i(s)\end{bmatrix}\begin{bmatrix}\Delta p_i(s)\\ \Delta q_i(s)\end{bmatrix}. \tag{4}$$

The device dynamics $D^{\mathrm{pf}}_i(s)$ and $D^{\mathrm{qv}}_i(s)$ allow for arbitrary rational transfer functions that capture decoupled pf- and qv-behavior. This model-agnostic representation accommodates a wide range of devices, including grid-forming VSCs and SGs, without relying on explicit parameterizations. Stacking all device models yields the overall device dynamics, i.e.,

$$-\begin{bmatrix}\Delta f(s)\\ \Delta|v|(s)\end{bmatrix} = \underbrace{\begin{bmatrix}D^{\mathrm{pf}}(s) & 0\\ 0 & D^{\mathrm{qv}}(s)\end{bmatrix}}_{=:\,D(s)}\begin{bmatrix}\Delta p(s)\\ \Delta q(s)\end{bmatrix} \tag{5}$$

where $D^{\mathrm{pf}}(s) = \mathrm{diag}(D^{\mathrm{pf}}_i(s))$ and $D^{\mathrm{qv}}(s) = \mathrm{diag}(D^{\mathrm{qv}}_i(s))$.

Interconnected Power System: The closed-loop power system is modeled as the feedback interconnection of the device dynamics (5) and the network dynamics (1), denoted by $D\#N$ (Fig. 2a). Due to the decoupling of device and network dynamics, this interconnection separates into pf- and qv-subsystems.

For stability analysis, we retain the full multi-node feedback interconnection to capture inter-node coupling. For performance analysis, we adopt reduced representations consistent with grid-code practice, namely the average-mode system frequency response of the pf-subsystem, and local voltage responses of the qv-subsystem. This enables the derivation of decentralized conditions on each $D^{\mathrm{pf}}_i(s)$ and $D^{\mathrm{qv}}_i(s)$, ensuring both closed-loop stability and performance of the overall power system.

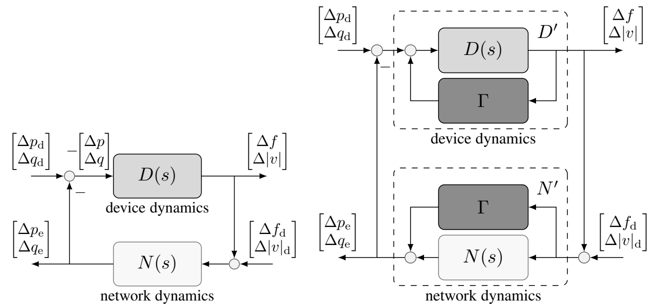

(a) Original feedback system. (b) Loop-shifted system with Γ.

Fig. 2: Closed-loop power system with active and reactive power disturbances Δp_{d} and Δq_{d}, and frequency and voltage disturbances Δf_{d} and $\Delta|v|_{\mathrm{d}}$.

Average-Mode System Frequency: Assuming stability of the pf-subsystem, the closed-loop mapping from active-power disturbances to frequency deviations is characterized by the network Laplacian. Its eigenvalue decomposition reveals that the dominant low-frequency behavior is governed by the coherent (average-mode) system frequency response, i.e.,

$$\Delta f_{\mathrm{avg}}(s) \approx \underbrace{\left(\textstyle\sum_{i=1}^{n}\left(D^{\mathrm{pf}}_i(s)\right)^{-1}\right)^{-1}}_{=:\,D_{\mathrm{avg}}(s)} \underbrace{\textstyle\sum_{i=1}^{n}\Delta p_{\mathrm{d},i}(s)}_{=:\,\Delta p^{\Sigma}_{\mathrm{d}}(s)}. \tag{6}$$

III. Device-Level Certification Methods

A. Stability Certification Criteria

By applying loop-shifting and passivity-based arguments as in [9], we derive decentralized device-level conditions that ensure internal feedback stability of the closed-loop interconnection $D\#N$. In particular, since the network transfer matrix $N(s)$ is not inherently passive, we introduce a block-diagonal loop-shifting matrix $\Gamma = \mathrm{diag}(0_{n\times n}, \Gamma^{\mathrm{qv}})$, leading to the loop-shifted interconnection $D'\#N'$ in Fig. 2b. The $n \times n$ matrix

$$\Gamma^{\mathrm{qv}} = \mathrm{diag}(c_i), \qquad c_i = \textstyle\sum_{j\neq i}^{n} b_{ij}\frac{0.8}{1+\rho^2}\frac{1}{|v|_{0,i}}, \tag{7}$$

is selected such that the loop-shifted network $N'(s)$ is passive [9]. The corresponding loop-shifted device dynamics $D'(s)$ are

$$D'(s) = \begin{bmatrix}D^{\mathrm{pf}}(s) & 0\\ 0 & D^{\mathrm{qv}}(s)(I - \Gamma^{\mathrm{qv}}D^{\mathrm{qv}}(s))^{-1}\end{bmatrix}. \tag{8}$$

Internal stability of $D'\#N'$ (and hence $D\#N$) follows if $D'(s)$ is strictly passive and a mild small-gain condition at $\omega = \infty$ holds [9]. Because (8) is diagonal, the conditions separate into independent constraints for the pf- and qv-channels.

Frequency control: Strict passivity and the small-gain condition of $D^{\mathrm{pf}}(s)$ reduce, for each device i, to

$$D^{\mathrm{pf}}_i(s) \text{ is stable and strictly proper,} \tag{1-i}$$

$$\mathrm{Re}[D^{\mathrm{pf}}_i(\mathrm{j}\omega)] > 0, \quad \forall\omega\in[0,\infty). \tag{1-ii}$$

Voltage control: Strict passivity and the small-gain condition of the loop-shifted qv-dynamics $D^{\mathrm{qv}}(s)(I - \Gamma^{\mathrm{qv}}D^{\mathrm{qv}}(s))^{-1}$ are guaranteed if each device i satisfies

$$D^{\mathrm{qv}}_i(s) \text{ is stable and strictly proper,} \tag{2-i}$$

$$c_i < \mathrm{Re}[D^{\mathrm{qv}}_i(\mathrm{j}\omega)^{-1}], \quad \forall\omega\in[0,\infty). \tag{2-ii}$$

If all devices satisfy conditions (1-i), (1-ii), (2-i), and (2-ii), then the overall interconnection $D\#N$ is internally stable.

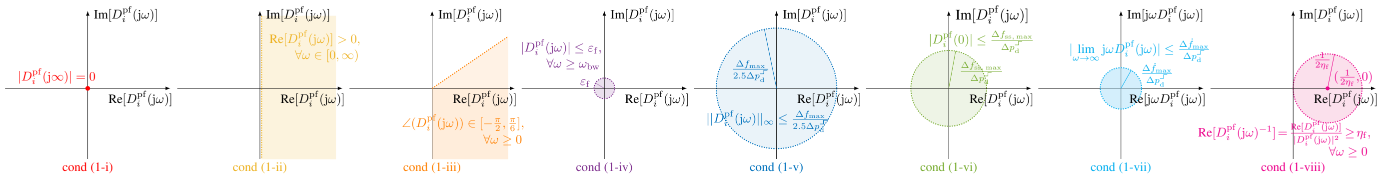

Fig. 3: Qualitative graphical illustration of the eight frequency-domain conditions (1-i) to (1-viii) for each $D_i^{\rm pf}(\mathrm{j}\omega)$ in the complex plane.

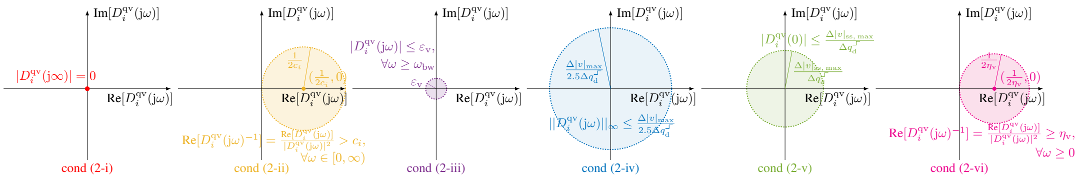

Fig. 4: Qualitative graphical illustration of the six frequency-domain conditions (2-i) to (2-vi) for each $D_i^{\rm qv}(\mathrm{j}\omega)$ in the complex plane.

B. Performance Certification Criteria

Frequency Control: Performance limits are imposed on the average-mode frequency response in (6) expressed through time-domain metrics after a worst-case active-power step disturbance $\Delta p_{\rm d}^{\sum}(s) = \frac{1}{s}\Delta p_{\rm d}^{\lrcorner}$. The considered time-domain metrics include a bounded nadir $\sup_{t\geq 0}|\Delta f_{\rm avg}^{\lrcorner}(t)| \leq \Delta f_{\max}$, a bounded steady-state deviation $|\lim_{t\to\infty}\Delta f_{\rm avg}^{\lrcorner}(t)| \leq \Delta f_{\rm ss,\,max}$, a bounded RoCoF $\sup_{t\geq 0}|\Delta \dot f_{\rm avg}^{\lrcorner}(t)| \leq \Delta \dot f_{\max}$, and sufficiently damped oscillations of $\Delta f_{\rm avg}^{\lrcorner}(t)$. These time-domain metrics are derived through a technically involved analysis exploiting properties of the Fourier integral and related algebraic arguments taken from [12]. Specifically, it can be shown that suitable decentralized constraints on each $D_i^{\rm pf}(s)$ enforce corresponding structural properties of the aggregate transfer function $D_{\rm avg}(s)$, which in turn imply the time-domain metrics on $\Delta f_{\rm avg}^{\lrcorner}(t)$. The full proof is omitted due to space limitations; instead, the resulting local conditions are summarized below. In particular, the *performance objectives* for $\Delta f_{\rm avg}^{\lrcorner}(t)$ are ensured if each device satisfies (1-i) and (1-ii), together with:

$$\angle(D_i^{\rm pf}(\mathrm{j}\omega)) \in [-\tfrac{\pi}{2}, \tfrac{\pi}{6}], \quad \forall\omega \geq 0, \tag{1-iii}$$
$$|D_i^{\rm pf}(\mathrm{j}\omega)| \leq \varepsilon_{\rm f}, \quad \forall\omega \geq \omega_{\rm bw}, \tag{1-iv}$$
$$||D_i^{\rm pf}(\mathrm{j}\omega)||_\infty \leq \frac{\Delta f_{\max}}{2.5\Delta p_{\rm d}^{\lrcorner}}, \tag{1-v}$$
$$|D_i^{\rm pf}(0)| \leq \frac{\Delta f_{\rm ss,\,max}}{\Delta p_{\rm d}^{\lrcorner}}, \tag{1-vi}$$
$$|\lim_{\omega\to\infty}\mathrm{j}\omega D_i^{\rm pf}(\mathrm{j}\omega)| \leq \frac{\Delta \dot f_{\max}}{\Delta p_{\rm d}^{\lrcorner}}, \tag{1-vii}$$
$$\mathrm{Re}[D_i^{\rm pf}(\mathrm{j}\omega)^{-1}] \geq \eta_{\rm f}, \quad \forall\omega \geq 0. \tag{1-viii}$$

Here, $\omega_{\rm bw}$ is a prescribed bandwidth, $\varepsilon_{\rm f} \approx 0$ enforces roll-off for $\omega \geq \omega_{\rm bw}$, and $\eta_{\rm f} > 0$ is an output feedback passivity index selected to ensure adequate damping. Conditions (1-iii), (1-iv) and (1-v) bound the nadir, (1-vi) bounds the steady-state deviation, (1-vii) bounds RoCoF, and (1-viii) enforces oscillation damping. A graphical illustration of the frequency-domain conditions (1-i) to (1-viii) is provided in Fig. 3.

Voltage Control: In the qv-subsystem there is no meaningful average mode; instead, voltage deviations are predominantly local. Accordingly, we approximate

$$\Delta|v|_i(s) \approx D_i^{\rm qv}(s)\Delta q_{{\rm d},i}(s), \tag{9}$$

and impose local time-domain bounds on the peak and steady-state voltage deviations, i.e., $\sup_{t\geq 0}|\Delta|v|_i^{\lrcorner}(t)| \leq \Delta|v|_{\max}$ and $|\lim_{t\to\infty}\Delta|v|_i^{\lrcorner}(t)| \leq \Delta|v|_{\rm ss,\,max}$, together with sufficient damping, under a worst-case reactive-power step $\Delta q_{{\rm d},i}(s) = \frac{1}{s}\Delta q_{\rm d}^{\lrcorner}$. These time-domain bounds are guaranteed if each device satisfies the conditions in (2-i) and (2-ii) and:

$$|D_i^{\rm qv}(\mathrm{j}\omega)| \leq \varepsilon_{\rm v}, \quad \forall\omega \geq \omega_{\rm bw}, \tag{2-iii}$$
$$||D_i^{\rm qv}(\mathrm{j}\omega)||_\infty \leq \frac{\Delta|v|_{\max}}{2.5\Delta q_{\rm d}^{\lrcorner}}, \tag{2-iv}$$
$$|D_i^{\rm qv}(0)| \leq \frac{\Delta|v|_{\rm ss,\,max}}{\Delta q_{\rm d}^{\lrcorner}}, \tag{2-v}$$
$$\mathrm{Re}[D_i^{\rm qv}(\mathrm{j}\omega)^{-1}] \geq \eta_{\rm v}, \quad \forall\omega \geq 0. \tag{2-vi}$$

Here, $\varepsilon_{\rm v} \approx 0$ enforces roll-off beyond $\omega_{\rm bw}$, and $\eta_{\rm v} > 0$ is chosen to ensure adequate damping. A graphical illustration of conditions (2-i) to (2-vi) is provided in Fig. 4. The proof parallels the frequency case, but applies directly to $D_i^{\rm qv}(s)$.

IV. Next-Generation Grid Code Specifications

Based on the derived stability and performance conditions, we formulate *Next-Generation Grid Code (NGGC)* specifications for frequency and voltage regulation: Each generation unit shall implement its pf- and qv-control via transfer functions $D_i^{\rm pf}(s)$ and $D_i^{\rm qv}(s)$ that satisfy the decentralized conditions in (1-i) to (1-viii) and (2-i) to (2-vi), respectively. Compliance with these specifications guarantees closed-loop stability and system-wide performance. The NGGC requirements admit an intuitive graphical interpretation in the complex plane, exemplarily illustrated by the Nyquist-plot envelopes in Fig. 5 for the pf-control (with an analogous interpretation for the qv-control).

V. Numerical Experiment

To validate the proposed NGGC framework and its stability and performance guarantees, we conduct numerical experiments in MATLAB/Simulink using a simple two-node system with two devices interconnected by an RL line. The setup follows the modeling assumptions of the NGGC framework: a quasi-stationary phasor-based network model is used, and only outer-loop device dynamics are implemented, neglecting inner converter loops and fast synchronous-machine dynamics. The numerical studies evaluate established generation-unit controls, including grid-forming VSCs and synchronous generators (SGs), with respect to the proposed NGGC conditions. We focus on the pf-subsystem while fixing all bus voltages at 1 p.u.

In the *first experiment*, one node uses a VSC with feasible control $D_1^{\rm pf}(s)$ (satisfying conditions (1-i)–(1-viii)), while the device under test (DUT) at the second node is varied. The DUTs include static droop (DUT 1), virtual oscillator control (VOC) (DUT 2), virtual synchronous machine (VSM) (DUT 3), generalized second-order droop control (DUT 4), and SGs

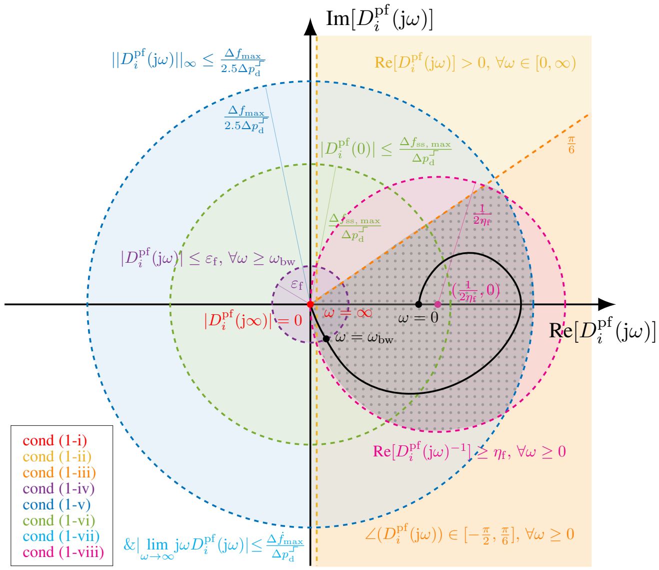

Fig. 5: Superposition of NGGC conditions (1-i) to (1-viii) in Fig. 3. The gray shaded region indicates the feasible set for all $\omega \in (0, \omega_{\mathrm{bw}})$, and the black curve depicts an exemplary feasible Nyquist plot of $D_i^{\mathrm{pf}}(\mathrm{j}\omega)$.

with non-reheat steam (DUT 5), reheat steam (DUT 6), and hydro turbines (DUT 7) (parameters from [13]). Their Nyquist characteristics and NGGC compliance are summarized in Fig. 6 and Table I. A 0.1 p.u. active-power step disturbance is applied at the DUT node, and the resulting average-mode frequency responses are shown in Fig. 7a. All configurations remain stable, consistent with approximate satisfaction of the strict passivity conditions (1-i) and (1-ii). While the steady-state frequency deviation remains within the ENTSO-E limit $\Delta f_{\mathrm{ss,max}} = 0.2$ Hz for all DUTs (condition (1-vi) satisfied), the frequency nadir correlates strongly with $\|D_2^{\mathrm{pf}}(s)\|_\infty$. Although SG-based DUTs 5-7 violate condition (1-v), the ideal VSC at node 1 limits the nadir well below the ENTSO-E bound $\Delta f_{\max} = 0.8$–1 Hz. RoCoF behavior and oscillation damping are consistent with conditions (1-vii) and (1-viii), respectively, where DUT 1&2 and DUT 4, violating condition (1-vii), exhibit the highest RoCoF values, even exceeding the ENTSO-E limit of $\Delta\dot{f}_{\max} = 2$ Hz/s.

In the *second experiment*, both nodes are equipped with identical DUTs. The corresponding frequency responses in Fig. 7b exhibit markedly degraded performance: the nadir exceeds the ENTSO-E limit for DUT 7 (violation of conditions (1-iii) and (1-v)), RoCoF constraints are violated for DUT 1&2 and DUT 4 (violation of condition (1-vii)), and pronounced oscillations appear for SG-based DUTs 5-7 (violation of condition (1-viii)). Overall, these results demonstrate that the proposed NGGC conditions capture key stability and performance trends and provide meaningful guidance for device-level control design.

VI. Conclusion

This paper presented preliminary results toward a decentralized, frequency-domain framework for certifying stability and performance in *Next-Generation Grid Codes*. The approach provides an initial, model-agnostic basis for linking local device behavior to system-level stability and performance. Ongoing work is extending these findings through larger-scale numerical studies with detailed network and device models, which will also investigate the dynamic behavior of the qv-subsystem.

	(1-i)	(1-ii)	(1-iii)	(1-iv)	(1-v)	(1-vi)	(1-vii)	(1-viii)
DUT 1 & 2	×	✓	✓	×	✓	✓	×	✓
DUT 3	✓	✓	✓	✓	✓	✓	✓	✓
DUT 4	✓	✓	✓	×	✓	✓	×	✓
DUT 5	✓	×	×	✓	×	✓	✓	×
DUT 6	✓	✓	×	✓	×	✓	✓	×
DUT 7	✓	×	×	✓	×	✓	✓	×

TABLE I: NGGC compliance of the different DUT control laws $D_2^{\mathrm{pf}}(s)$.

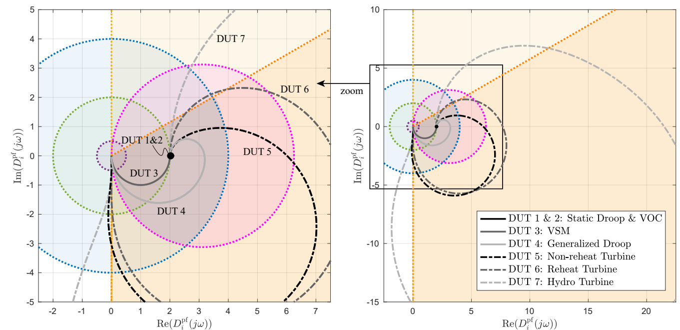

Fig. 6: Nyquist plots of the DUT controllers $D_2^{\mathrm{pf}}(s)$, with NGGC conditions indicated using the same colors as in Fig. 5.

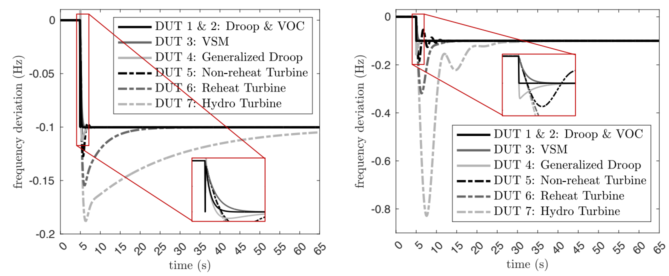

(a) First experiment. (b) Second experiment.

Fig. 7: Average-mode frequency responses of the two-node test system.

VII. AI Usage Disclosure

We have been using AI (Chat GPT Plus) for spell- and grammar-checking, and style improvements of this paper.

References

[1] "Commission regulation (EU) 2016/631 of 14 april 2016, establishing a network code on requirements for grid connection of generators," tech. rep., European Commission, 2016.

[2] "The technical requirements and the prequalification process of fast frequency reserve (ffr)," tech. rep., Oyj, Fingrid, 2021.

[3] "Techn. Anforderungen an Netzbildende Eigenschaften inkl. der Bereitstellung von Momentanreserve," tech. rep., VDE FNN Hinweis, 2024.

[4] D. Groß, "Compensating network dynamics in grid-forming control," in *58th Annual Allerton Conference on Communication, Control, and Computing (Allerton)*, 2022.

[5] H. Geng, X. Xi, and G. Yang, "Small-signal stability of power system integrated with ancillary-controlled large-scale DFIG-based wind farm," *IET Renewable Power Generation*, vol. 11, no. 8, pp. 1191–1198, 2017.

[6] "Technical requirements for frequency containment reserve provision in the nordic synchronous area," tech. rep., ENTSO-E, 2022.

[7] A. Hoke *et al.*, "White paper: Grid forming functional specifications for bps-connected battery energy storage systems," tech. rep., North American Electric Reliability Corporation (NERC), 2023.

[8] Z. Siahaan, E. Mallada, and S. Geng, "Decentralized stability criteria for grid-forming control in inverter-based power systems," in *IEEE Power & Energy Society General Meeting*, 2024.

[9] V. Häberle, X. He, L. Huang, F. Dörfler, and S. Low, "Decentralized parametric stability certificates for grid-forming converter control," *arXiv preprint arXiv:2503.05403*, 2025.

[10] L. Huang, D. Wang, X. Wang, H. Xin, P. Ju, K. H. Johansson, and F. Dörfler, "Gain and phase: Decentralized stability conditions for power electronics-dominated power systems," *IEEE Transactions on Power Systems*, vol. 39, no. 6, pp. 7240–7256, 2024.

[11] L. Huang, L. Luo, R. Leng, H. Xin, D. Wang, and F. Dörfler, "Geometric decentralized stability condition for power systems based on projecting dw shells," *arXiv:2508.17033*, 2025.

[12] A. Papoulis, *The Fourier Integral and its Applications*. McGraw-Hill, New York, 1962.

[13] P. Kundur, *Power System Stability and Control*. McGraw-Hill, 1994.

I. REVIEW #88A

A. Paper summary

This submission presents a passivity-like methodology for stability certification of power/frequency, reactive power/voltage local dynamic behavior of generators connected to a power system network. The presentation describes the conceptual basis of the approach and illustrates its application with results on two numerical examples comparing various generator types and their compliance/non-compliance of their frequency-domain conditions and the ensuing time-domain responses.

B. Comments for authors

The paper is very interesting and appears as a compelling contribution to discussion on future interoperability generator requirements embodying stability in modern power systems. The four pages of the submission only permit a rather brief summary of the approach – details and proofs of the proposed conditions appearing elsewhere. It is unclear how conservative these conditions can be, although some degree of conservativeness in characterising dynamic interoperability across a diverse range of generators. The paper is clearly presented with clever use of colour-coding matching mathematical conditions and high-quality visualisations.

C. Summarize your recommendation in one to two sentences

I recommend the paper be accepted for presentation at the conference. The evolution of grid-codes in power systems to incorporate rigorous universal conditions for interconnected stability is an important area for development and a welcome contribution.

— Julio Braslavsky

II. REVIEW #88B

A. Paper summary

This paper presents preliminary results aimed at a reimagined framework for grid codes based in frequency-domain criteria (e.g., passivity, small-gain, small-phase, etc.), Instead of standard time-domain metrics (e.g., nadir, RoCoF, settling time, etc.).

B. Comments for authors

Strengths:

- [+] Well written and relatively easy to follow, especially considering the control-theoretic of contributions
- [+] Connecting proposed frequency-domain criteria to standard time-domain ones
- [+] Nice use of colours to visualize various proposed frequency-domain conditions via graphical interpretation

Weaknesses:

- [-] While I commend authors for the ambitious undertaking to completely rework existing standards and codes, I worry that this may be too far removed from what might be practically feasible.
- [-] I am not fully convinced that there is a real need for the proposed framework. At the moment, the simulations seem to demonstrate that there is a one-to-one correspondence between existing time-domain metrics and proposed frequency-domain ones. Results could be strengthened by demonstrating improvement of proposed metrics in some way.

C. Summarize your recommendation in one to two sentences

This is a well-written paper aimed at an ambitious undertaking of reimagining grid codes. I recommend for the paper to be accepted.

— Anonymous reviewer

III. REVIEW #88C

A. Paper summary

The paper designs grid codes for converters providing ancillary services. They start with a linear model in which real power is coupled to frequency and reactive power to voltage magnitude. They use the model to define device-level stability certificates for frequency and voltage. They also use the model to define performance certificates for criteria like frequency nadir and RoCoF. There is nice illustration of the conditions in figures, and a two bus numerical example examining which conditions are satisfied by various control laws.

B. Comments for authors

The paper is well-written and the technical content is interesting and logical. The term 'next generation grid code' strikes me as a poor choice, as 'next generation' won't be valid in the future, and tells us nothing about the grid code.

C. *Summarize your recommendation in one to two sentences*

The paper is well written and technically interesting.

— Anonymous reviewer

IV. Brief response to reviewers (optional)

We sincerely thank all reviewers for their positive evaluations, constructive comments, and recommendation for acceptance. We are pleased that the reviewers found the paper technically interesting, well written, and relevant to the discussion on future interoperability requirements and grid codes.

Regarding Reviewer 88A, we appreciate the positive assessment. We agree that the conservatism of the proposed conditions is an important question. A systematic study of conservatism is beyond the scope of this four-page paper and is part of our ongoing and future work.

Regarding Reviewer 88B, we agree that our vision is ambitious. Our intention is not to propose a one-to-one replacement of today's grid codes, but rather to inspire a future framework based on decentralized frequency-domain certificates. This direction is consistent with recent developments, such as the use of Nyquist-based criteria in the Nordic countries or passivity requirements, e.g., in Finland. We also emphasize that the main novelty is not merely establishing a correspondence between frequency- and time-domain metrics, but providing **decentralized** certificates that guarantee **global** closed-loop stability and performance of the interconnected system. Existing grid codes prescribe **global** time-domain limits (e.g., COI frequency metrics) without requiring **local** device-level conditions that ensure these global objectives are achieved.

Regarding Reviewer 88C, we thank the reviewer for the positive feedback. We appreciate the suggestion regarding the title. We intentionally retain the wording ”next generation grid code” to emphasize the forward-looking perspective of the paper, although we acknowledge that alternative terminology may be appropriate in future, more comprehensive publications.

V. Brief summary of changes made to the final paper

No changes made, except for correcting one typo in equation (7).